On-line measurement of magnetic susceptibility for titanium minerals processing

By G Cavanough[1] and P N Holtham[2]

ABSTRACT

Magnetic separation is routinely used in the processing of titanium minerals, and the efficiency of these operations can be determined by measuring the magnetic properties of the process streams. The valuable components in the feed to a titanium minerals plant have specific magnetic susceptibilities ranging from -10^{-9} m^3 kg^{-1} (zircon) to 10^{-6} m^3 kg^{-1} (ilmenite). However, in an industrial environment, in which the mineral temperature may range from 20 to 120°C, it is difficult to measure susceptibilities lower than about 10^{-7} m^3 kg^{-1}. Hence laboratory testing of spot samples from magnetic separators is currently required to obtain accurate performance data. This is an inherently slow process and where feed grades are variable, optimum performance of magnetic separators is generally not achieved.

This paper describes the development of an inductance-based instrument for measuring very low levels of magnetic susceptibility on-line. The signal from the instrument can be used for process control purposes to maintain optimum magnetic separator performance.

A prototype instrument has been installed in the zircon scavenger circuit in an Australian titanium minerals plant. The circuit consists of a roll magnetic separator treating a feed consisting mainly of monazite and stained zircon. The monazite-rich magnetic fraction is returned to the mine site for disposal, while the non-magnetic fraction is recycled to the zircon wet circuit. Splitter positions in the separator are adjusted when the final zircon product fails to meet specification, or the magnetic fraction contains more than 30 per cent zircon. Weekly composite grain counts show that sub-optimal operation of the magnetic separator results in significant zircon losses into the magnetics fraction.

Using the instrument, the zircon content of this stream can now be accurately determined from the measured magnetic susceptibility, provided a correction for the effect of mineral temperature is applied using the Curie - Weiss relationship.

INTRODUCTION

The separation of titanium minerals by electrical and magnetic methods has been an active area of research at the Julius Kruttschnitt Mineral Centre (JKMRC) for over 20 years. This work has identified the need for a device to measure the magnetic susceptibility of minerals on-line (Stradling, 1991). It would allow monitoring, control and optimisation of magnetic separation processes. It might also find application in electrostatic separation, as a means of measuring iron staining.

A variety of techniques is available to measure magnetic susceptibility including inductance, magnetic force, vibrating a sample in a magnetic field, rotating a magnetic field in the presence of a sample and SQUID (Foner, 1981; Svoboda, 1987; Sepulveda, Thomas and Wikswo, 1994).

However, the production environment dictates that the inductance method is the most suitable due to it being inexpensive, immune to vibration and able to give a real-time measurement. In inductance measurement, the magnetic properties of a sample are determined from the change in impedance of a coil due to the presence of the sample.

DESIGN SPECIFICATION

From a review of the relevant literature and inspection of plant operating environments the following specifications were adopted:

1. Senior Research Officer, Julius Kruttschnitt Mineral Research Centre, Isles Road, Indooroopilly Qld 4068.

2. Principal Research Fellow, Julius Kruttschnitt Mineral Research Centre, Isles Road, Indooroopilly Qld 4068. E-mail: p.holtham@mailbox.uq.edu.au

- The required level of sensitivity in measurement is 10^{-9} m^3 kg^{-1}.

  The components of feed to a titanium minerals plant have specific magnetic susceptibilities, ranging from -10^{-9} to 10^{-5} m^3 kg^{-1} (Table 1). Numerous measurements are available for minerals with susceptibilities down to 10^{-7} m^3 kg^{-1} (Collinson, 1983; Exelby, 1992; Isokangas, 1996; Svoboda, 1987), but comparatively few results were found for materials of lower susceptibilities. Errors due to sample presentation, temperature, stray magnetic fields and inherent electronics noise were reported as limiting sensitivity (Foner, 1981; Collinson, Creer and Runcorn, 1967) and may be the reason for the lack of results for lower magnetic susceptibility minerals. All AC induction measurement devices described in the literature were operated in a laboratory environment. Consequently, it may be difficult to measure magnetic susceptibilities of less than 10^{-7} m^3 kg^{-1} in an industrial environment;

- The device must be able to operate in ambient temperatures ranging from 0°C to 70°C with the operating temperature changing by ±10°C;

- Accurate measurement must be maintained when measuring mineral streams at temperatures ranging from 20°C to 120°C with the operating temperature changing by ±10°C. Therefore temperature correction will be required using the Curie - Weiss law (Stradling, 1991);

- The device must be a flow through design as valve arrangements have limited life in titanium minerals plants;

- The cost of an on-line measurement device must be low. Titanium minerals plants utilise large numbers of magnetic separators requiring installation of many devices;

The design of a suitable instrument can be broken into two major tasks. Task 1 is the design of the electronic circuitry to supply current to the coil and then measure the impedance change of the coil due to the presence of a mineral sample. The difficulty of this task is significantly reduced if the coil is able to produce a high signal to noise ratio. Consequently Task 2, the design of the coil to maximise the signal to noise ratio, will be the focus of this paper.

TABLE 1

Major components of feed material to a titanium minerals plant.

Mineral	Approximate Magnetic Susceptibility
Ilmenite FeTiO$_3$	10^{-6} m^3 kg^{-1}
Leucoxene FeTiO$_3$ .TiO$_2$	10^{-7} m^3 kg^{-1}
Rutile TiO$_2$	10^{-8} m^3 kg^{-1}
Zircon ZrSiO$_4$	-10^{-9} m^3 kg^{-1}
Monazite (Ce, La, Y, Th)PO$_4$	10^{-7} m^3 kg^{-1}
Staurolite FeO.Al$_2$O$_3$ .SiO$_4$	10^{-6} m^3 kg^{-1}
Kyanite Al$_2$O$_3$ .SiO$_2$	-10^{-10} m^3 kg^{-1}
Garnet (Ca, Mg, Fe, Mn) SiO$_4$	10^{-7} m^3 kg^{-1}
Quartz SiO$_2$	-10^{-10} m^3 kg^{-1}

COIL DESIGN

Initial work

Initial experimental work was carried out using copper wire induction coils in a standard bridge system. This work identified temperature drift as the main source of measurement error. The temperature change induced by simply breathing on the coils would cause an immediate change in the output. Copper wire has a 0.39 per cent change in resistance per °C (Schofield, 1982) and is therefore the dominant cause of the drift.

A review of the literature suggested that a send/receive coil system as opposed to the simple bridge circuit would provide measurements independent of coil resistance (Anon, 1981). Hence a send/receive coil system was adopted for the design.

The send/receive coil system is shown in Figure 1. As the receive coils are wound in opposition to each other there is no output when the coils are empty. When a sample is placed in one coil, the magnetic properties of the sample change the flux linkage between the send and receive coils producing an output voltage ($V_{receive}$) proportional to the change ($\phi_1 - \phi_2$).

Temperature drift is eliminated by negating effects caused by changes in coil resistance. This is achieved in the send coil by maintaining a constant current and hence a constant magnetic flux, while in the receive coil the very high input impedance amplifier renders changes in coil resistance insignificant.

A sinusoidal AC voltage is applied to the send coil. It follows that the output is also sinusoidal. The magnetic properties of the sample will change the amplitude of the sinusoidal output and may also shift the phase as shown in Figure 2.

FIG 1 - Send/receive coil schematic and assembly.

Collinson (1983), and Tarling and Hrouda (1993) showed that there would be amplitude change resulting from samples having the levels of magnetic susceptibility of titanium minerals but phase shift would be negligible (the value of negligible was not specified). The present authors consider that the phase information may be of value in identification of mineral species and hence it was included in the instrument design specification.
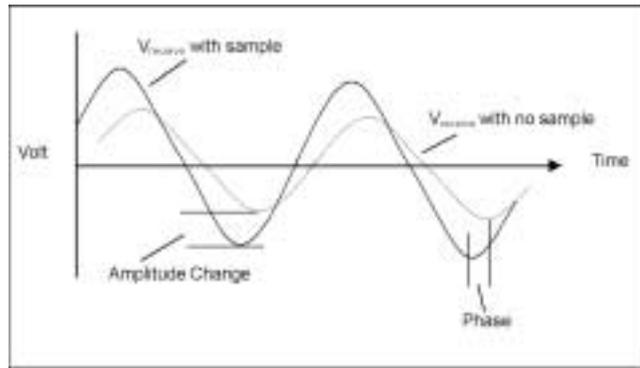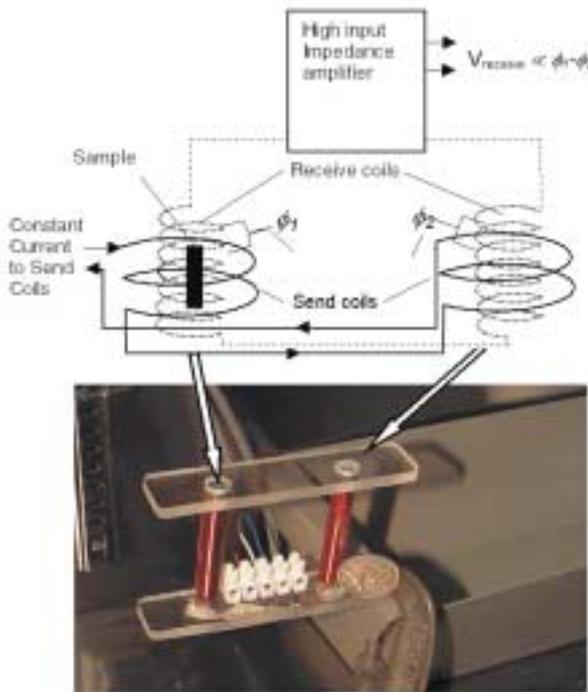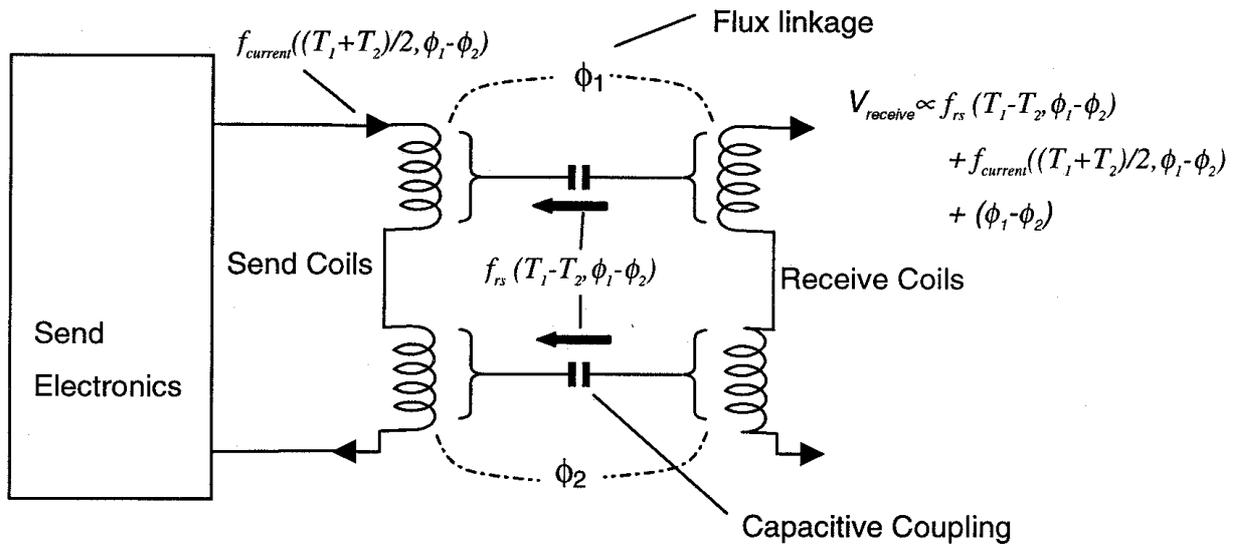

FIG 2 - Change in $V_{receive}$ caused by magnetic properties of the sample.

Chemical salts and minerals were used to calibrate the amplitude change in units of magnetic susceptibility.

Two tests were then carried out on the coil assembly to determine if the send/receive configuration did eliminate temperature drift. In the first test the entire coil assembly was heated from 20 to 40°C and the change in amplitude (in units of magnetic susceptibility) and phase of the receive coil voltage were recorded. This test mimics ambient temperature changes of the entire coil assembly. The results of this test were a 0.033×10^{-7} m^3 kg^{-1} amplitude change and a -1.35° phase shift.

In the second test only one coil was heated from 20 to 40°C (the other coil was kept at 20°C) and the change recorded. This test mimics normal operating conditions in which hot mineral flows through one coil while the other coil is at ambient temperature. The results were a 2.41×10^{-7} m^3 kg^{-1} amplitude change and a -0.43° phase shift.

The change in phase with temperature shows that the nominally constant current to the send coil was also being changed in phase. The presence of a sample may also change the phase of the constant current. Therefore it is likely that the instrument will produce an erroneous phase measurement.

The design specifies temperature variations of ±10°C with a resolution of 10^{-9} m^3 kg^{-1} and results from Test 1 are within this specification. This was expected as the coils are arranged in a bridge type configuration so if both coils are at the same temperature then balance is maintained. Test 2, a true representation of normal operation, resulted in temperature drift that was 200 times greater than specification.

In order to identify the reasons for the temperature drift it was necessary to develop a detailed model of the coil system. The model is described in the next section.

MODELING THE SEND/RECEIVE COIL

Figure 3 shows a schematic of the send/receive coil system identifying two possible sources of temperature drift: change in phase of the send coil current, and coupling of flux linkage current from receive to send coil. When these sources are included, the ideal equation for the receive coil output voltage $V_{receive} \propto (\phi_1 - \phi_2)$ becomes:

$$V_{receive} \propto f_{rs}(T_1 - T_2, \phi_1 - \phi_2) + f_{current}((T_1+T_2)/2, \phi_1 - \phi_2) + (\phi_1 - \phi_2)$$

where: T_1 and T_2 are the temperatures of coil 1 and coil 2, $f_{rs}(T_1 - T_2, \phi_1 - \phi_2)$ is the function representing current flow from the receive coil to the send coil via capacitive coupling and $f_{current}((T_1+T_2)/2, \phi_1 - \phi_2)$ is the function representing the phase change of the theoretically constant current supplied to the send coil.

The formulation of each of these functions is described in the following sections.

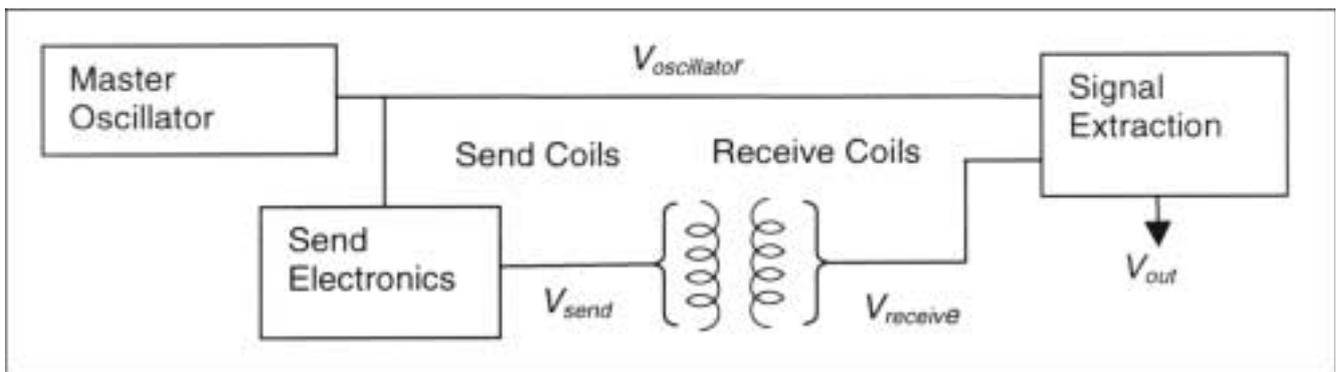FIG 3 - Schematic of send/receive coil sources of temperature drift.

FIG 4 - Representation of the send/receive coil and circuit.

The temperature drift due to the change in phase of the send coil current

Derivation

This source of temperature drift arises from the inability of the send electronics to control the phase of the constant current supplied to the send coils. Constant current is maintained by controlling the amplitude of the voltage to the send coil (ie as the temperature rises the coil resistance will rise. To maintain a constant current the send electronics will increase the voltage). This is an AC voltage hence the current has both phase and amplitude of which only the amplitude is controlled. Figure 4 is a representation of the coil and circuit identifying the significant voltages. It also shows the Master Oscillator and Signal Extraction circuit sections.

All AC voltages used in the circuit are derived from the master oscillator. Consequently, all phase and amplitude changes in $V_{receive}$ are relative to this voltage.

The signal extraction circuit converts $V_{receive}$ to a DC voltage using a multiplier and low pass filter as follows:

$$V_{oscillator} = A\ cos(\omega t)$$

and

$$V_{receive} = B\ cos(\omega t + \theta)$$

where B is the amplitude and θ is the phase (refer to Figure 3).

Multiplying the two voltages gives:

$$AB/2\ [cos(2\omega t + \theta) + cos(\theta)]$$

Low pass filtering of this voltage gives:

$AB/2\ [cos(\theta)]$ – this should be constant regardless of temperature.

Temperature drift is described as follows:

- $V_{oscillator}$ never changes. Therefore A is a constant;

- The function of the send circuit is to keep the send coil current (and hence $V_{receive}$) constant regardless of the impedance of the coil (which changes with temperature) by varying V_{send}. However, coil impedance is complex making V_{send} out of phase with coil current, ie $V_{send} = C\ cos(\omega t + \theta)$ (with both C and θ changing with coil temperature);

- This means that the amplitude and phase of V_{send} will change with respect to $V_{receive}$. As V_{send} is derived from $V_{oscillator}$ it follows that the phase of $V_{oscillator}$ must change with temperature. This gives the circuit output as:

$V_{send} = K \cos(\theta)$ where K is a constant and θ is temperature dependent.

$f_{current}((T_1+T_2)/2, \phi_1 - \phi_2)$ is a phase shift of $V_{receive}$ and is determined from the change in the phase angle of the impedance of the send coil:

$$f_{current}((T_1+T_2)/2, \phi_1 - \phi_2) = \text{phase of } Z_{send \text{ at temperature 2}} - \text{phase of } Z_{send \text{ at temperature 1}}.$$

Solution

Drift due to $f_{current}((T_1+T_2)/2, \phi_1 - \phi_2))$ was overcome by implementing the following signal extraction algorithm in the electronic circuit (modified circuit shown in Figure 5):

- A signal $V_{current} = C \cos(\omega t)$ is derived from the send coil current and is therefore always in the same phase relationship as the flux linkage;

- Taking $V_{receive} = B \cos(\omega t + \theta)$ where B is the amplitude and θ is the phase (refer Figure 2);

- Phase and amplitude are extracted as follows;

$V_{receive} \times V_{receive}$

$= B \cos(\omega t + \theta) \times B \cos(\omega t + \theta)$

with filtering $= B^2/2 = S_{receive}$

$V_{current} \times V_{current}$

$= C \cos(\omega t + \theta) \times C \cos(\omega t + \theta)$

with filtering $= C^2/2 = S_{current}$

$V_{receive} \times V_{current}$

$= B \cos(\omega t + \theta) \times C \cos(\omega t + \theta)$

with filtering $= (BC/2) \cos(\theta) = S_{rec \times cur}$

Therefore the amplitude of $V_{receive}$ is: $\sqrt{2 S_{receive}}$

and the phase angle is: $cos^{-1}\left(\dfrac{S_{rec \times cur}}{\sqrt{S_{receive} \times S_{current}}} \right)$ radians

The original signal extraction algorithm gave a measured phase shift of -1.35° and a calculated phase shift of -1.21°. Implementation of the modified algorithm resulted in zero phase shift.

The temperature drift due to coupling of flux linkage current from receive to send coil

Derivation

The voltage at the receive coil ($V_{receive}$) is due to the flux linkage between the send and receive coils. Ideally the receive coil is an open circuit and no current will flow. In reality capacitive coupling does form a circuit and there is a flow of current via the coupling to the send coil. Figure 6 shows the circuit for the current flowing from the receive to the send coil via the capacitive coupling. $V_{receive}$, due to $f_{rs}(T_1 - T_2, \phi_1 - \phi_2)$ is calculated as follows:

$$f_{rs}(T_1 - T_2, \phi_1 - \phi_2) =$$

$$V_{receive} = V_{linkage}(Z1_{coupling}/(Z1_{receive}+Z_{coupling})) - V_{linkage}(Z2_{coupling}/(Z2_{receive}+Z_{coupling})).$$

where $Z1_{receive}$, $Z2_{receive}$, $Z1_{coupling}$ and $Z2_{coupling}$ are the changes in impedance of the coils and capacitive coupling due to temperature drift (Z_{send} is ignored because $Z_{coupling} \gg Z_{send}$).

Solution

It is evident from these equations that if the coil assembly is at a uniform temperature then there would be no $V_{receive}$ due to temperature drift. This agrees with the temperature test results which show the drift is negligible when both coils are at the same temperature. The obvious solution is to keep the coils at the same temperature. Using the Test 2 results of a drift of 2.41×10^{-7} m^3 kg^{-1} for a 20°C change in temperature, equates to keeping the coils within 0.1°C of each other to keep the level of drift within design specification. Clearly this is not economically viable in an industrial environment.

The next obvious solution is to use a material between the send and receive coils that has a dielectric constant that does not change with temperature. This would result in a constant capacitive coupling impedance. To-date such a material, that is also suitable for coil construction, has not been found.

The third option was to increase the impedance of the capacitive coupling between the coils by increasing the separation between the send and receive coils. A new coil assembly was constructed using a 1 mm gap between the send and receive coils. Polystyrene was used to form the layer.

Unexpectedly, the drift increased to a value of 2.71×10^{-7} m^3 kg^{-1} for a 'Test 2' type test of the new coil. Investigation revealed that when the new coils were fabricated the dimension of the gap between the coils was not uniform. This resulted in the coils not matching - which means that $\phi_1 - \phi_2$ has a significant value when the coils are empty. Consequently the gain of the measurement system must be decreased to keep the output from saturating. The gain used in the new coil was nine per cent of the gain used in the original coil. When this value was used in the calculation the result agreed with the measured value. This exercise did not produce a superior coil – however it did validate the model, ie $f_{rs}(T_1 - T_2, \phi_1 - \phi_2)$.

The final option considered and the simplest solution is to use batch operation. This is achieved by stopping mineral flow through the coil with a valve assembly, and taking a reading with the coil empty to use as a dynamic reference level. Although this option was excluded in the design specification, it had to be reconsidered as it offered a complete solution to temperature drift and hence would be a benchmark to which other solutions could be compared. A valve assembly was designed using an actuator from a car central locking system. Valve cost was kept below $10 with a plentiful supply of spare parts and an estimated life of one year. A prototype instrument and batch valve system was constructed and installed in a titanium minerals plant.
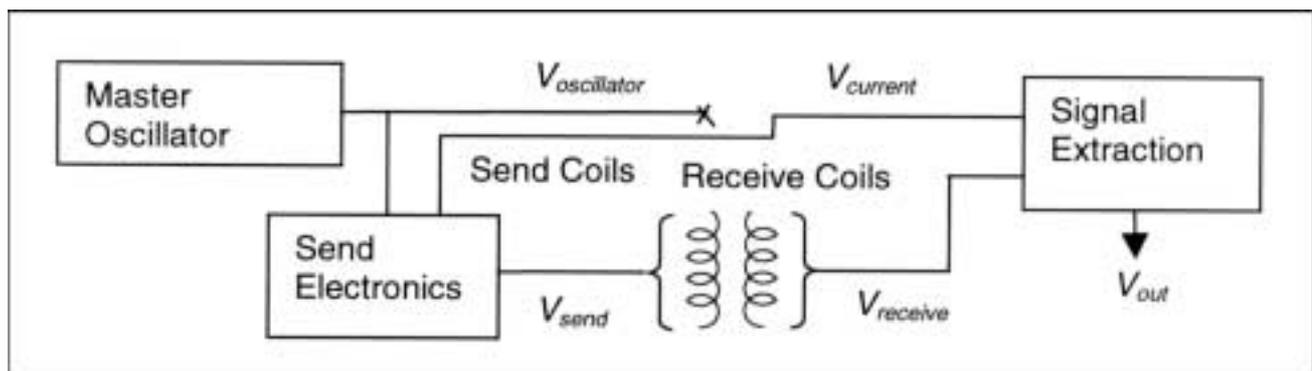

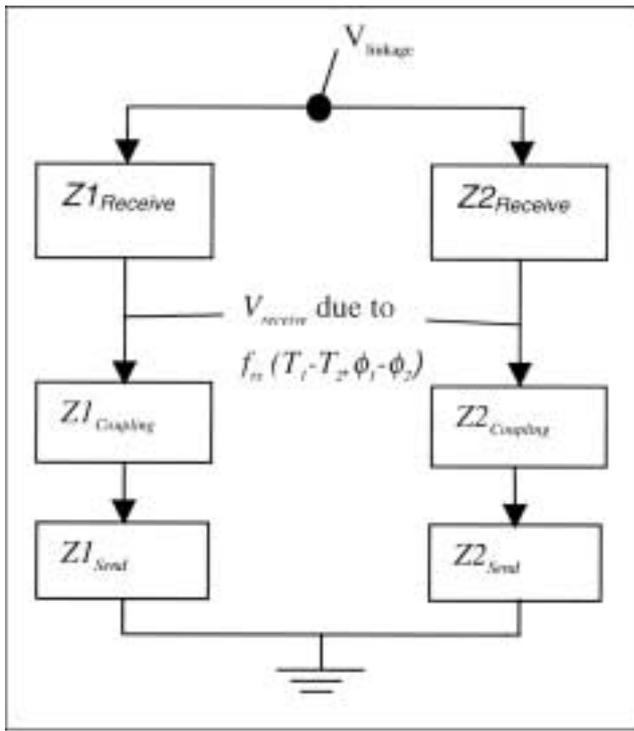FIG 5 - Representation of the send/receive coil and modified circuit.

FIG 6 - Calculation of f_{rs} $(T_1 - T_2, \phi_1 - \phi_2)$.

INSTALLATIONS IN A TITANIUM MINERALS PLANT

The on-line measurement device was installed in the zircon magnetics circuit of a titanium minerals plant. This circuit consists of a scavenger roll magnetic separator used to clean the zircon in a tailings stream consisting of mainly monazite and stained zircon. The device was installed in the magnetic stream out of the separator in series with an automatic sampler (with sample cuts taken every six minutes and stored for weekly analysis).

Separator splitter position is used to adjust the zircon recovery. Adjustment is made when either the zircon product does not conform to specification or the zircon magnetics sample contains greater than 30 per cent zircon (the automatically collected sample is analysed weekly by performing a laboratory separation and grain count). It is estimated that 600 tonnes of zircon per year are currently lost to the magnetics stream. Hence, significant financial gains will result from a real time measurement of the zircon component because it would allow immediate adjustment of splitter position. Previously analysed zircon magnetics samples were run through the prototype instrument to ascertain whether the magnetic properties were correlated with the amount of zircon in the samples.

The instrument is measuring the susceptibility of the magnetics stream, which is inversely proportional to the zircon concentration. Figure 7 shows the calibrated correlation between per cent zircon and the magnetic susceptibility of the stream. It can be seen that as the level of zircon increases the overall magnetic susceptibility of the sample decreases as a result of low susceptibility zircon diluting the stream. There is also a relationship between phase angle measured by the prototype instrument and per cent zircon in the stream. However the magnitude of the magnetic susceptibility change (ie amplitude change) was far greater than the phase change. Therefore the magnetic susceptibility measurement had much better resolution and was used to calculate per cent zircon in the on-line instrument. Phase angle was recorded as it will be the focus of future work because it has been shown to be unaffected by temperature drift.

Magnetic susceptibility decreases with sample temperature and Stradling (1991) showed that temperature correction can be made using the Curie - Weiss relationship. To use this relationship the paramagnetic Curie temperature for the mineral must be determined by temperature testing. The paramagnetic Curie temperature is found by plotting a curve of the inverse of magnetic susceptibility as a function of temperature. By extrapolation the temperature at which inverse magnetic susceptibility is zero (the paramagnetic Curie temperature) can be determined. This method was used to find the paramagnetic Curie temperature of mineral stream flowing through the on-line instrument. Using this data it was calculated that per cent zircon reading had a temperature drift of approximately 0.5 per cent per °C. Hence, temperature correction was incorporated in the instrument.
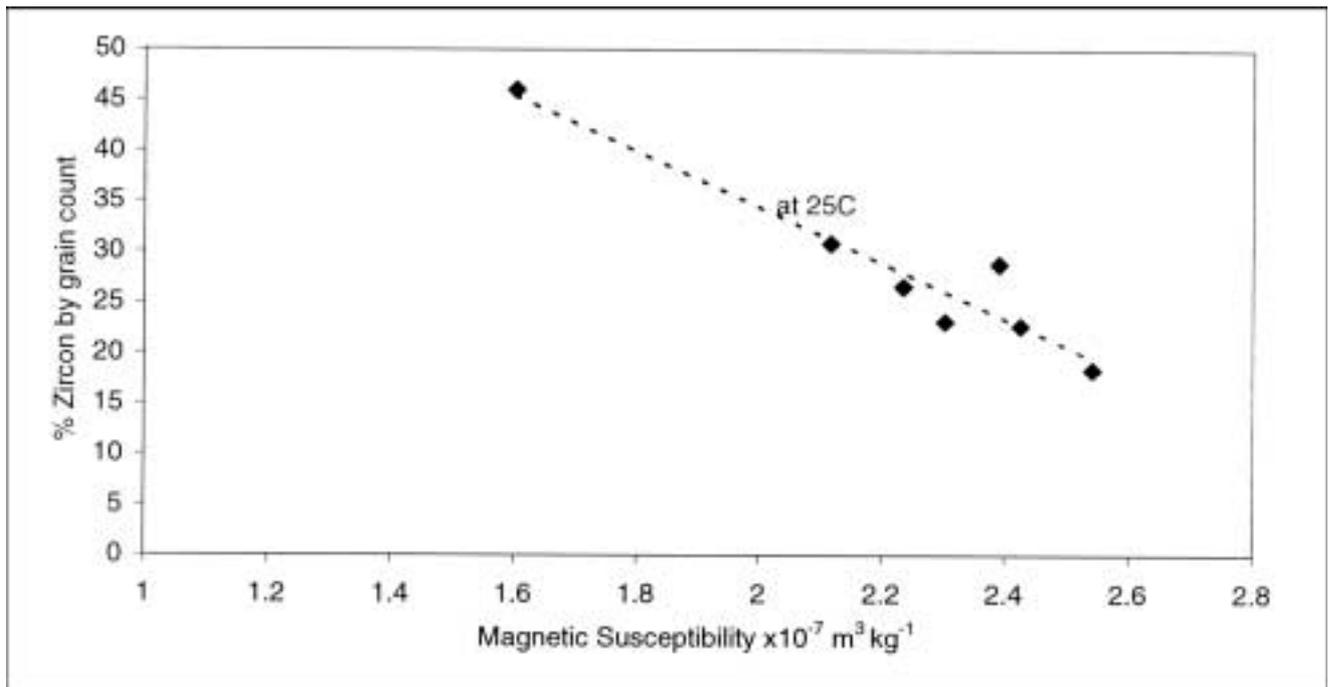

FIG 7 - Per cent zircon as a function of magnetic susceptibility.

TABLE 2

Comparison of instrument measurements and laboratory results.*

	Week 1	Week 2	Week 3	Week 4
% zircon from measurement	18	22	19	22
% zircon from laboratory analysis	19	23	18	22

* Table 2 - compares per cent zircon measurements taken by the measurement device with the laboratory results obtained from the samples collected by the automatic sampler.

Table 2 compares per cent zircon measurements taken by the measurement device with the laboratory results obtained from the samples collected by the automatic sampler.

CONCLUSION

Temperature drift of the coils has been identified as the major hurdle in the development of an on-line induction device to measure the magnetic properties of minerals. The literature suggested that the use of a send/receive coil configuration should overcome this error. In practice temperature drift occurs due to capacitive coupling between coils and phase shifting of the coil current.

Models of these phenomena have been developed and proven by experimentation. From these models a new signal extraction algorithm has been designed which negates the effect of the phase shifting. Solutions to the problem of temperature drift caused by capacitive coupling are progressing, with a batch system being implemented in the interim.

The prototype instrument has been installed in the zircon magnetics circuit of a titanium minerals plant. It has been found that the zircon content of the stream can be determined by the level of magnetic susceptibility. There is also a temperature independent relationship between the phase of the output voltage of the coil and the amount of zircon in the stream.

The system has been designed to output a real time measure of the zircon content of the mineral stream. This information is used to limit the loss of zircon and hence increase company revenue.

ACKNOWLEDGEMENTS

REFERENCES

Anon, 1981. Advance Manual for Eddy Current Test Methods (Canadian Government Standards Board).

Collinson, D W, 1983. *Methods in Rock Magnetism and Palaeomagnetism* (Chapman and Hall Ltd: London).

Collinson, D W, Creer, K M and Runcorn, K M, (Eds) 1967. *Developments in Solid Earth Geophysics* 3. Methods in Palaeomagnetism, (Elsevier Publishing Company: London).

Exelby, H R A, 1992. A model of the high gradient magnetic separator used for kaolin beneficiation, MSc Thesis (unpublished), University of Queensland, Brisbane.

Foner, S, 1981. Review of magnetometry, *IEEE Trans Mag*, 17(6):3358-3363.

Isokangas, E A, 1996. Aspects of Process Control in Mineral Sands Dry Plant, PhD Thesis (unpublished), University of Queensland, Brisbane.

Schofield, W, 1982. *Physical Science for Engineers* (McGraw - Hill Book Company (UK) Limited: Maidenhead, Berkshire England).

Sepulveda, N, Thomas, I and Wikswo, J, 1994. Magnetic susceptibility tomography for a three dimensional imaging of diamagnetic and paramagnetic objects, *IEEE Transactions on Magnetics,* 30:5062-5069.

Stradling, A, 1991. Mathematical Models of Dry High - Intensity Magnetic Separators, PhD Thesis (unpublished), University of Queensland, Brisbane.

Svoboda, J, 1987. *Magnetic Methods for the Treatment of Minerals* (Elsevier Science Publishers BV: Amsterdam).

Tarling, D H and Hrouda, F, 1993. *The Magnetic Anisotropy of Rocks* (Chapman and Hall: London).